J|A|C|S COMMUNICATIONS

Published on Web 02/27/2009

Catalyzed Hydrogen Spillover for Hydrogen Storage

Ralph T. Yang* and Yuhe Wang

Department of Chemical Engineering, University of Michigan, Ann Arbor, Michigan 48109

Received November 11, 2008; E-mail: yang@umich.edu

The use of hydrogen as the energy source for fuel-cell vehicles relies in part on the development of a viable hydrogen storage system. The U.S. Department of Energy (DOE) has established specific R&D targets for on-board hydrogen storage.[1] Among the most important targets are system gravimetric/volumetric capacities and charge/discharge rates.[1] Although there are currently a number of candidate storage materials, none is capable of meeting the DOE targets.[2] During the last six years, a new class of promising sorbent materials has been under development using the approach of hydrogen spillover.[3] The hydrogen spillover phenomenon, which is defined as dissociative chemisorption of H_2 on a metal and subsequent migration or surface diffusion of the atomic hydrogen onto the support surfaces, has long been observed on supported metal catalysts.[4] Although the storage capacities can be increased substantially by spillover, the rates of spillover are slow and remain a major concern.[3f] In the apparently unrelated development of metal hydrides for H_2 storage, the slow kinetics dictates the temperature that is required for charge and discharge. For this reason, intense studies on added catalysts have been undertaken. Since the 1960s, several organic compounds have been found to have catalytic effects on Mg.[5a] Addition of 1% Pd yielded significant catalytic effects on Mg_2Ni and $LaNi_5$.[5b] In 1997, it was discovered that doping of $NaAlH_4$ with $TiCl_3$ or $TiCl_4$ increased the rates in both directions several-fold.[5c] Subsequently, many other transition metals (e.g., cations of Zr, Fe, Mn, Cr, Co, and Nd) have also been found to be effective.[5d] Carbon was found to increase the rates for Mg[5e] and was also found to be a cocatalyst.[5f−h] Many studies on the Ti-catalyzed $NaAlH_4$ system have been carried out in order to gain an understanding of the catalytic mechanism.[5i−l] However, the mechanism remains unclear, although density functional theory analysis[5m] and muon spin resonance spectroscopy data[5n] indicate that hydrogen-related point defects and vacancies could be involved.

Here we report the significant catalytic effects of Ti and V chlorides on hydrogen spillover on Pt-doped carbon. A superactivated carbon, designated AX-21 [Brunauer−Emmet−Teller (BET) surface area = 2800 m^2/g, Anderson Development Co.), was used. The rates for both adsorption and desorption were significantly increased by doping with 2 wt % $TiCl_3$ or VCl_3. To our knowledge, this is the first time that catalytic effects have been observed for hydrogen spillover.

Pt nanoparticles were doped on AX-21 carbon through solution of H_2PtCl_6 in acetone aided by ultrasonication, followed by drying and reduction in H_2 at 300 °C for 2 h. Details are given elsewhere[3f] and in the Supporting Information. Pt/AX-21 was doped with 2 wt % $TiCl_3$ or VCl_3 via incipient wetness impregnation using solution in diethyl ether. The solvent was evaporated at 50 °C for 2 h, and the sample was heat-treated by degassing at 200 °C (or higher) for 12 h prior to H_2 adsorption measurements (see the Supporting Information). The BET surface areas of these samples are given in Table 1. They were measured by N_2 adsorption at −196 °C (77 K) using a Micromeritics ASAP 2020 system. The same system was also used for measuring low-pressure H_2 isotherms at <1 atm as well as rates of uptake at different temperatures in the same pressure range.

Table 1. Pt/AX-21 and Catalyst-Doped Pt/AX-21 BET Surface Areas (*A*) and Activation Energies for Spillover (ΔE) during a Pressure-Increase Step

sample	*A* (m^2/g)	pressure step (mmHg)	ΔE (kJ/mol)
Pt/AX-21	2521	65.0–74.0	7.5
Pt/AX-21+$TiCl_3$	2501	65.0–71.0	6.5
Pt/AX-21+VCl_3	2498	67.0–74.0	6.8

The high-pressure H_2 isotherms and rates for both adsorption and desorption were measured with a Sievert's apparatus. The system was fully calibrated and proven to be accurate. Details of the system are given elsewhere.[6] Isotherms at 25 °C for Pt/AX-21 and Pt/AX-21 doped with 2 wt % $TiCl_3$ are shown in Figure 1, and that for the VCl_3-doped sample is shown in Figure 2. For both the $TiCl_3$- and VCl_3-doped samples, the isotherms were lowered slightly, reflecting the slight reduction in the surface areas due to doping. The desorption branches are also shown. Interestingly, the

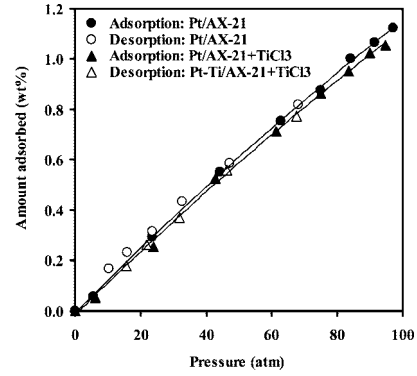

Figure 1. High-pressure isotherms for H_2 adsorption/desorption on Pt/AX-21 and Pt/AX-21+$TiCl_3$ at 25 °C.

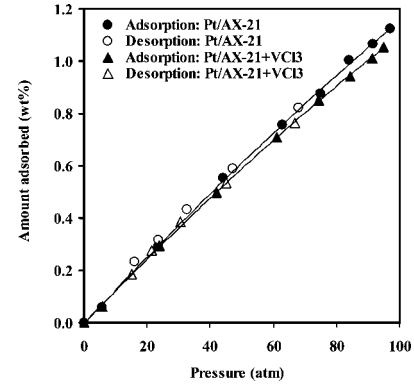

Figure 2. High-pressure isotherms of H_2 adsorption/desorption on Pt/AX-21 and Pt/AX-21+VCl_3 at 25 °C.

10.1021/ja808864r CCC: $40.75

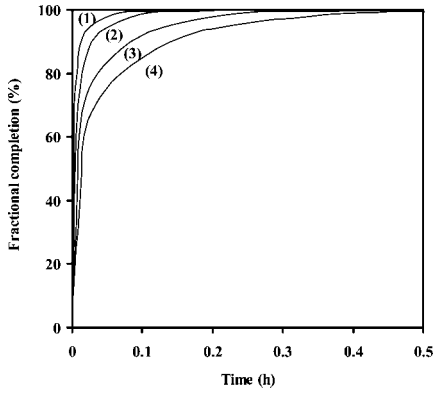

Figure 3. Rates of adsorption on Pt/AX-21 and Pt/AX-21+$TiCl_3$ at 25 °C and various pressures. Pressure steps: (1) 0−6.1 atm H_2 on Pt/AX-21+$TiCl_3$; (2) 0−5.7 atm H_2 on Pt/AX-21; (3) 6.1−24.0 atm H_2 on Pt/AX-21+$TiCl_3$; (4) 5.7−23.5 atm H_2 on Pt/AX-21.

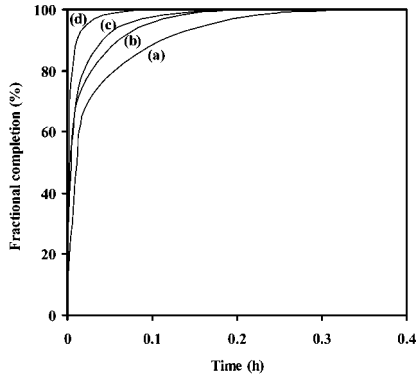

Figure 4. Rates of desorption on Pt/AX-21 and Pt/AX-21+$TiCl_3$ at 25 °C and various pressures. Pressure steps: (a) 32.8−23.5 atm for Pt/AX-21; (b) 31.9−21.9 atm for Pt/AX-21+$TiCl_3$; (c) 23.5−15.9 atm for Pt/AX-21; (d) 21.9−15.7 atm for Pt/AX-21+$TiCl_3$.

small adsorption/desorption hysteresis loop for Pt/AX-21 disappeared upon doping with $TiCl_3$ or VCl_3.

The uptake rates for both low-pressure (<1 atm) and high-pressure ranges (>1 atm) were significantly increased upon doping with 2 wt % $TiCl_3$. The high-pressure uptake rate data are shown in Figure 3 (the low-pressure uptake rate data will be shown later). The desorption rates for the $TiCl_3$-doped sample are shown in Figure 4. Again, doping with 2 wt % $TiCl_3$ significantly increased the desorption rates. As discussed elsewhere,[3f] the rates of both adsorption and desorption decreased at higher hydrogen loading, as seen here for all of the samples. Moreover, the desorption rates were higher than the adsorption rates, as also seen here.

The rates of both adsorption and desorption for the VCl_3-doped sample are compared with those of Pt/AX-21 in Figures 5 and 6. Here again the significant catalytic effects are seen.

Doping with $TiCl_3$ or VCl_3 was performed sequentially (i.e., the metal salt was doped after Pt nanoparticles were doped on AX-21 carbon). Codoping was also performed for $TiCl_3$, and the results were very similar to those for the sequentially doped sample. In this case, the $TiCl_3$ and Pt salt were doped from an ether solution. The results on codoped samples are given in the Supporting Information.

It has been shown that the rate-limiting step for the spillover process on these and similar samples near ambient temperature is surface diffusion on carbon.[3f−h,4] Also, it has been shown that H atoms are the diffusing species.[3f,h,4b,7] Thus, the surface diffusion process was catalyzed by doping with $TiCl_3$ or VCl_3.

In order to understand the catalytic mechanism, heats of adsorption and activation energies (ΔE) for surface diffusion (via

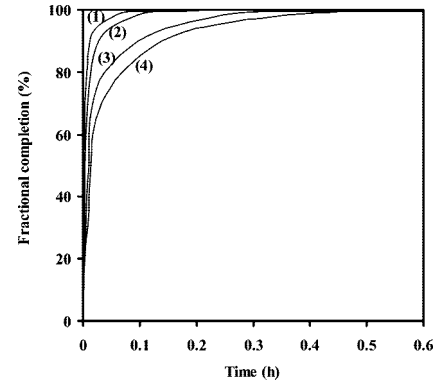

Figure 5. Rates of adsorption on Pt/AX-21 and Pt/AX-21+VCl_3 at 25 °C and various pressures. Pressure steps: (1) 0−5.8 atm H_2 on Pt/AX-21+VCl_3; (2) 0−5.7 atm H_2 on Pt/AX-21; (3) 5.8−23.8 atm H_2 on Pt/AX-21+VCl_3; (4) 5.7−23.5 atm H_2 on Pt/AX-21.

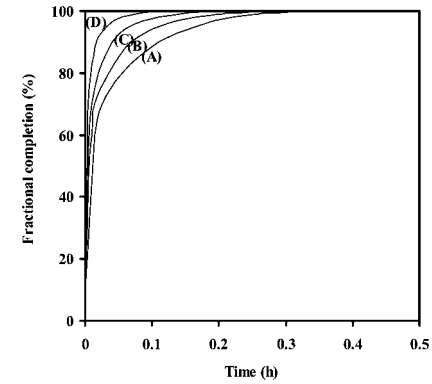

Figure 6. Rates of desorption from Pt/AX-21 and Pt/AX-21+VCl_3 at 25 °C and various pressures. Pressure step: (A) 32.8−23.5 atm for Pt/AX-21; (B) 30.6−21.4 atm for Pt/AX-21+VCl_3; (C) 23.5−15.9 atm for Pt/AX-21; (D) 21.4−15.0 atm for Pt/AX-21+VCl_3.

spillover rates) were obtained for all of the samples. The overall heats of adsorption were determined from the temperature dependence of the isotherms via the Clausius−Clapeyron equation, while the ΔE values for spillover were calculated from the temperature dependence of the uptake rates.

As mentioned earlier, the low-pressure (<1 atm) data on both isotherms and rates were obtained using a commercial Micromeritics 2020 sorptomer. The detailed data on the temperature dependence of the isotherms are given in the Supporting Information. The uptake rates at various temperatures in this pressure range were measured for all of the pressure increase steps, and for illustrative purposes, the results for one step are shown in Figures 7, 8, and 9.

The rates for both adsorption (spillover) and desorption (reverse spillover[3h]) at 298 K are high at low pressures (or low hydrogen loadings) and become increasingly smaller as the pressure increases. Figures 7−9 show the uptake rate data for comparable pressure increase steps for Pt/AX-21 and Pt/AX-21 doped with 2 wt % $TiCl_3$ or VCl_3. Again, the catalytic effects of these chlorides are clearly seen. From these rate data, estimates of the surface diffusion time constants[3f] D/R^2, where D is the surface diffusivity and R is an average radius of diffusion for spillover, were first made. To obtain the activation energy for surface diffusion, the following temperature dependence was used:

$$D = D_0 e^{-\Delta E/R'T} \quad (1)$$

where R' is the gas constant, T is the absolute temperature, and ΔE is the difference in energy between the states corresponding to adsorption at the ground vibrational level of the bond and to free mobility on the

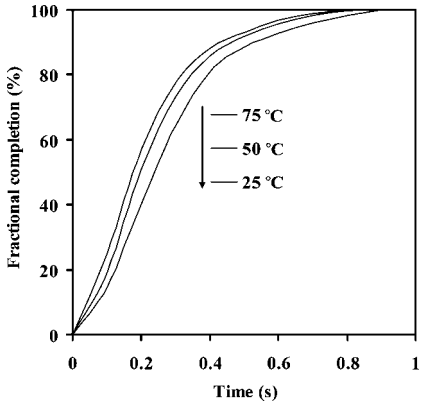

Figure 7. Rates of uptake of H_2 on Pt/AX-21 in the 65.0−74.0 mmHg H_2 pressure increase step at 25, 50, and 75 °C.

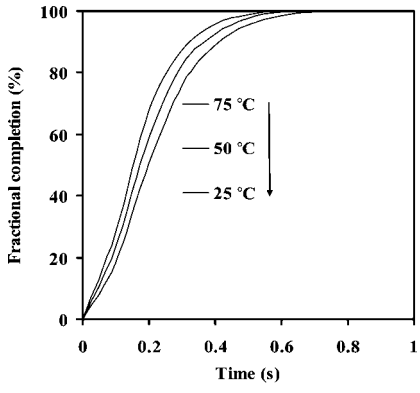

Figure 8. Rates of uptake of H_2 on Pt/AX-21+$TiCl_3$ in the 65.0−71.0 mmHg H_2 pressure increase step at 25, 50, and 75 °C.

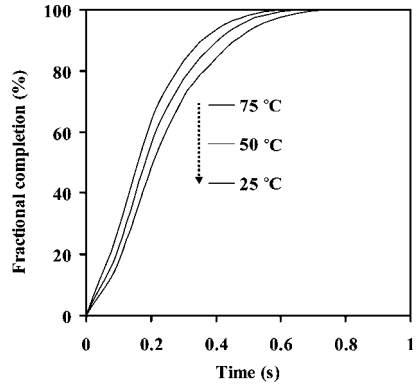

Figure 9. Rates of uptake of H_2 on Pt/AX-21+VCl_3 in the 67.0−74.0 mmHg H_2 pressure increase step at 25, 50, and 75 °C.

surface. Thus, plots of $\log(D/R^2)$ versus $1/T$ yielded the activation energies.

The results for the heats of adsorption are shown in Figure 10, and the ΔE values are given in Table 1. Both the heats of adsorption and the values of ΔE for spillover were decreased significantly by doping with $TiCl_3$ or VCl_3. This result indicates that the binding energies between the spilled-over H and the sites on carbon surfaces were decreased by doping. The activation energy for surface diffusion is typically a fraction of the binding energy;[8] a decrease in the binding energy would result in a decrease in the activation energy and would consequently lead to higher diffusion rates. Apparently, the catalytic effects observed for spillover in this study are unrelated to those for metal hydrides, which are considerably stronger. Further studies on the mechanism, both theoretical and

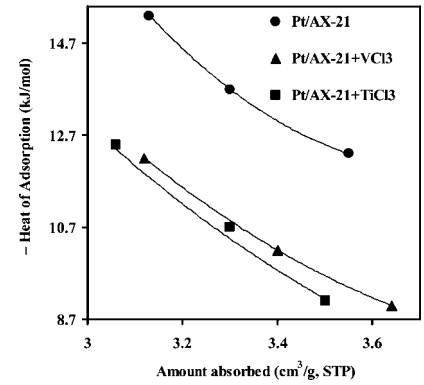

Figure 10. Overall isosteric (exothermic) heats of adsorption for undoped and doped samples.

experimental, are in progress. Likewise, the effects of other catalysts for hydrogen spillover are being studied.

Acknowledgment. The authors acknowledge the funding provided by the U.S. Department of Energy's Office of Energy Efficiency and Renewable Energy within the Hydrogen Sorption Center of Excellence (HS CoE) as well as funding from NSF.

Note Added after ASAP Publication. The version published Feb 27, 2009 contained errors in Figures 1, 2, and S1. The corrected version was published Mar 9, 2009.

Supporting Information Available: Experimental details, Pt/AX-21+VCl_3 data, and isotherms at low pressure and at various temperatures. This material is available free of charge via the Internet at http://pubs.acs.org.

References

(1) (a) U.S. Department of Energy, Energy Efficiency and Renewable Energy (EERE), Hydrogen, Fuel Cells & Infrastructure Technologies Program, Multi-Year RD&D Plan, 2005. (b) Satyapal, S.; Petrovic, J.; Read, C.; Thomas, G.; Ordaz, G. *Catal. Today* **2007**, *120*, 246–256.
(2) (a) Dillon, A. C.; Heben, M. J. *Appl. Phys. A: Mater. Sci. Process.* **2001**, *72*, 133–142. (b) Züttel, A. *Mater. Today* **2003**, *6*, 24–33.
(3) (a) Yang, R. T.; Li, Y. W.; Qi, G.; Lachawiec, A. J. U.S. Patent Appl. US20070082816A1, filed 2005. (b) Lueking, A.; Yang, R. T. *J. Catal.* **2002**, *206*, 165–168. (c) Lachawiec, A. J.; Qi, G.; Yang, R. T. *Langmuir* **2005**, *21*, 11418–11424. (d) Li, Y. W.; Yang, R. T. *J. Am. Chem. Soc.* **2006**, *128*, 726–727. (e) Li, Y. W.; Yang, R. T. *J. Am. Chem. Soc.* **2006**, *128*, 8136–8137. (f) Li, Y. W.; Yang, R. T. *J. Phys. Chem. C* **2007**, *111*, 11086–11094. (g) Wang, L.; Yang, R. T. *J. Phys. Chem. C* **2008**, *112*, 12486–12494. (h) Lachawiec, A. J., Jr.; Yang, R. T. *Langmuir* **2008**, *24*, 6159–6165.
(4) (a) Robell, A. J.; Ballou, E. V.; Boudart, M. *J. Phys. Chem.* **1964**, *68*, 2748–2753. (b) Conner, W. C.; Falconer, J. L. *Chem. Rev.* **1995**, *95*, 759–788.
(5) (a) Zaluska, A.; Zaluski, L.; Strom-Olsen, J. O. *J. Alloys Compd.* **1999**, *288*, 217–225. (b) Zaluski, L.; Zaluska, A.; Tessier, P.; Strom-Olsen, J. O.; Schulz, R. *J. Alloys Compd.* **1995**, *217*, 295–300. (c) Bogdanovic, B.; Schwickardi, M. *J. Alloys Compd.* **1997**, *253*−*254*, 1–9. (d) Anton, D. L. *J. Alloys Compd.* **2003**, *356*, 400–404. (e) Wang, J.; Ebner, A. D.; Zidan, R.; Ritter, J. A. *J. Alloys Compd.* **2005**, *391*, 245. (f) Wu, C. Z.; Wang, P.; Yao, X.; Lu, G. Q.; Cheng, H. M. *J. Phys. Chem. B* **2005**, *109*, 22217–22221. (g) Yao, X.; Wu, C. Z.; Du, A. J.; Wang, P.; Lu, G. Q.; Cheng, H. M.; Smith, S. C.; Zou, J.; He, Y. *J. Phys. Chem. B* **2006**, *110*, 11697–11703. (h) Wang, J.; Ebner, A. D.; Ritter, J. A. *J. Phys. Chem. B* **2006**, *110*, 17353–17358. (i) Gross, K. J.; Sandrock, G.; Thomas, G. J. *J. Alloys Compd.* **2002**, *330*−*332*, 691–695. (j) Gross, K. J.; Thomas, G. J.; Jensen, C. M. *J. Alloys Compd.* **2002**, *330*−*332*, 683–690. (k) Ozolins, V.; Majzoub, E. H.; Udovic, T. J. *J. Alloys Compd.* **2004**, *375*, 1–10. (l) Løwik, O. M.; Opalka, S. M. *Phys. Rev. B* **2005**, *71*, 054103. (m) Peles, A.; Van de Walle, C. G. *Phys. Rev. B* **2007**, *76*, 214101. (n) Kadono, R.; Shimomura, K.; Satoh, K. H.; Takeshita, S.; Koda, A.; Nishiyama, K.; Akiba, E.; Ayabe, R. M.; Kuba, M.; Jensen, C. M. *Phys. Rev. Lett.* **2008**, *100*, 026401.
(6) Lachawiec, A. J.; DiRaimondo, T. R.; Yang, R. T. *Rev. Sci. Instrum.* **2008**, *79*, 063906.
(7) (a) Mitchell, P. C. H.; Ramirez-Cuesta, A. J.; Parker, S. F.; Tomkinson, J.; Thompsett, D. *J. Phys. Chem. B* **2003**, *107*, 6838–6845. (b) Mitchell, P. C. H.; Ramirez-Cuesta, A. J.; Parker, S. F.; Tomkinson, J. *J. Mol. Struct.* **2003**, *651*−*653*, 781–785.
(8) (a) Sladek, K. J.; Gilliland, E. R.; Baddour, R. F. *Ind. Eng. Chem. Fundam.* **1974**, *13*, 100–105. (b) Kapoor, A.; Yang, R. T.; Wong, C. *Catal. Rev.*−*Sci. Eng.* **1989**, *31*, 129–214.

JA808864R